Table I. IR Bands and Their Assignments for Complex **1** and Its Photoproduct (**2**)[a]

complex	solvent	temp, °C	ν(C≡O)	ν(NO)	$\nu(\mathrm{C{=}O})^{\alpha}_{\mathrm{cis}}$	$\nu(\mathrm{C{=}O})^{\beta}_{\mathrm{cis}}$	$\nu(\mathrm{C{=}O})^{\alpha}_{\mathrm{trans}}$	$\nu(\mathrm{C{=}O})^{\beta}_{\mathrm{trans}}$
1	2-MeTHF	−140	2007	1755	1590	1666	1605	1619
1	CH_2Cl_2	−100	2015	1758	1590	1662	1605	1612
2	2-MeTHF	−140		1708	1590	1648	1605	1561
2	CH_2Cl_2	−100		1707	1590	1648	1605	1555

[a] Values in cm^{-1}.

complexes,[2] the s-cis isomer is presumed to have the larger energy separation between the bands assigned to the α-carbonyl ($\nu(\mathrm{C{=}O})^{\alpha}$) and β-carbonyl ($\nu(\mathrm{C{=}O})^{\beta}$) groups of the ligand, with the lower energy band in each isomer assigned to the α-carbonyl. Figures 1 and 2 present the IR spectral changes accompanying the photoreaction of **1** in CH_2Cl_2 at −100 °C and in 2-MeTHF at −140 °C, respectively.

Discussion

Irradiation of complex **1** with the 436-nm line of a medium-pressure mercury lamp induced loss of the CO ligand as evidenced by the disappearance of the metal carbonyl band at 2007/2015 cm^{-1} and the growth of the IR band of free CO (2134 cm^{-1} in CH_2Cl_2, 2131 cm^{-1} in 2-MeTHF). The nitrosyl band ν(NO) shifted to lower frequency with the same value observed for both isomers. It is noteworthy that the IR bands assigned to the α-carbonyl groups of the α-ketoacyl ligand in both the s-cis and s-trans isomers do not shift during the reaction whereas the bands due to the β-carbonyl groups are very sensitive to the loss of CO, especially that of the s-trans isomer. Its frequency shifts by more than 50 cm^{-1} to lower energy whereas $\nu(\mathrm{C{=}O})^{\beta}_{\mathrm{cis}}$ only shifts by ~15 cm^{-1}. Upon warming of the irradiated solutions, back-reaction occurred beginning at ~−100 °C to re-form the original isomers of the α-ketoacyl complex **1**, but the spectra did not permit a determination of which isomer reacted faster.

The interpretation of these results is straightforward. The frequency lowering of ν(NO) is caused by the increase of π-back-bonding after loss of CO. The open site created by this reaction is apparently not occupied by a solvent molecule, since the IR bands of the photoproduct hardly differ in CH_2Cl_2 and 2-MeTHF. The latter is known to be a good coordinating solvent at −140 °C.[3] It is therefore proposed that in both isomers this open site is occupied by some part of the α-ketoacyl ligand. The lack of an observed shift in the IR bands assigned to the α-carbonyl groups of the two isomers indicates that these groups do not occupy the coordination site. For the s-trans isomer, the β-carbonyl of the α-ketoacyl ligand is favorably oriented for coordination of the carbonyl oxygen (Scheme I) and such coordination is indicated by the large photoinduced shift of the IR band assigned to the β-carbonyl of this isomer. For the s-cis isomer, we suggest that the coordination site opened by photoejection of CO is either weakly coordinated by the tolyl group, as indicated in Scheme I, or is unoccupied.

The low-temperature photolysis results presented above are consistent with the observation that room-temperature photolysis of complex **1** in the presence of PPh_3 does not lead to CO deinsertion but rather to clean photosubstitution of PPh_3 for CO (eq 1). The above results suggest that intermediates like those shown in Scheme I may be produced in the latter photosubstitution reaction and may thus stabilize the "open" coordination site until PPh_3 displaces the coordinated α-ketoacyl ligand in an S_N2-type reaction.

Acknowledgment. G. Schoemaker is thanked for technical assistance with the IR measurements. This work was supported in part by the U.S. Department of Energy, Office of Basic Energy Sciences.

---

(2) (a) Casey, C. P.; Bunnell, C. A.; Calabrese, J. C. *J. Am. Chem. Soc.* **1976**, *98*, 1166. (b) Chen, J.; Sen, A. *J. Am. Chem. Soc.* **1987**, *109*, 148. (c) Ozawa, F.; Sugimoto, T.; Yuasa, Y.; Santra, M.; Yamamoto, T.; Yamamoto, A. *Organometallics* **1984**, *3*, 683. (d) Ozawa, F.; Sugimoto, T.; Yamamoto, T.; Yamamoto, A. *Organometallics* **1984**, *3*, 692. (e) Fayos, J.; Dobrzynski, E.; Angelici, R. J.; Clardy, J. *J. Organomet. Chem.* **1973**, *59*, C33. (f) Bochmann, M.; Hawkins, L.; Hursthouse, M. B.; Short, R. L. *J. Organomet. Chem.* **1987**, *332*, 361. (g) des Abbayes, H. *New J. Chem.* **1987**, *11*, 535.

(3) See, for example: van Dijk, H. K.; Stufkens, D. J.; Oskam, A.; Rotteveel, M.; Heijdenrijk, D. *Organometallics* **1987**, *6*, 1665.

Contribution from the Department of Chemistry,
Purdue University, West Lafayette, Indiana 47907-3699

Conversion of $[ReH(acac)_2(PPh_3)_2]PF_6$ to *cis*-$[Re(acac)_2(PPh_3)_2]PF_6$ through a Coupled Oxidation/Deprotonation Reaction

Malee Leeaphon, Phillip E. Fanwick, and Richard A. Walton*

Received May 14, 1990

Introduction

In the course of a recent study in which we examined the reactivity of $ReH_7(PPh_3)_2$ toward various donor ligands, we reported the syntheses and structures of the Re(IV)–Re(III) redox pair $[ReH(acac)_2(PPh_3)_2]PF_6$ and $ReH(acac)_2(PPh_3)_2$, where acac is the anion of 2,4-pentanedione.[1] The Re(IV) salt $[ReH(acac)_2(PPh_3)_2]PF_6$ is obtained by a simple one-electron oxidation of the neutral Re(III) complex $ReH(acac)_2(PPh_3)_2$. When further oxidation of the Re(IV) complex was attempted, a monohydride Re(V) complex was not formed; instead, a new Re(III) cation was produced through the deprotonation of the unstable species $[ReH(acac)_2(PPh_3)_2]^{2+}$. In this report, we describe the formation of *cis*-$[Re(acac)_2(PPh_3)_2]PF_6$ (**1**) from the reaction of $[ReH(acac)_2(PPh_3)_2]PF_6$ with the oxidant $NOPF_6$. The crystal structure of **1** is also reported, thereby permitting a structural comparison to the previously reported structures of the precursor complexes, $[ReH(acac)_2(PPh_3)_2]PF_6$ and $ReH(acac)_2(PPh_3)_2$, as well as to other six-coordinate, mononuclear acetylacetonate complexes of rhenium.

Experimental Section

General Procedures. All reactions were performed under an atmosphere of dry nitrogen. All solvents were thoroughly deoxygenated prior to use. The compounds $ReH(acac)_2(PPh_3)_2$ and $[ReH(acac)_2(PPh_3)_2]PF_6$ were prepared by methods described elsewhere.[1] Both $NOPF_6$ and 1,8-diazabicyclo[5.4.0]undec-7-ene (DBU) were obtained from commercial sources. All reagents and solvents were obtained from commercial sources.

Infrared spectra were recorded in the range 4000–450 cm^{-1} as Nujol mulls between KBr plates on a Perkin Elmer Model 1800 IR Fourier transform spectrometer. Electronic absorption spectra were recorded in the range 900–300 nm on an IBM Instruments 9420 UV–visible spectrophotometer. Cyclic voltammetric measurements were carried out by the use of a Bioanalytical Systems Inc. Model CV-1A instrument on dichloromethane solutions that contained 0.1 M tetra-*n*-butylammonium hexafluorophosphate (TBAH) as the supporting electrolyte. $E_{1/2}$ values, determined as $(E_{p,a} + E_{p,c})/2$, were referenced to the silver/silver chloride (Ag/AgCl) electrode at room temperature and are uncorrected for junction potentials. Under our experimental conditions the ferrocenium/ferrocene couple is at $E_{1/2} = +0.47$ V vs Ag/AgCl. Bulk electrolyses

---

(1) Fanwick, P. E.; Leeaphon, M.; Walton, R. A. *Inorg. Chem.* **1990**, *29*, 676.

0020-1669/90/1329-4348$02.50/0

Table I. Crystallographic Data for *cis*-[Re(acac)$_2$(PPh$_3$)$_2$]PF$_6$ (**1**)

chemical formula	ReP$_3$F$_6$O$_4$C$_{46}$H$_{44}$	Z	4
		T, °C	20
fw	1053.97	radiation (λ, Å)	Mo Kα (0.71073)
space group	$P2_1/c$ (No. 14)	ρ_{calcd}, g cm^{-3}	1.560
a, Å	10.815 (1)	μ(Mo Kα), cm^{-1}	29.13
b, Å	19.725 (2)	transm coeff	1.00–0.82
c, Å	21.063 (2)	R^a	0.029
β, deg	92.634 (9)	$R_w{}^b$	0.039
V, Å^3	4488 (1)		

[a] $R = \sum||F_o| - |F_c||/\sum|F_o|$. [b] $R_w = \{\sum w(|F_o| - |F_c|)^2/\sum w|F_o|^2\}^{1/2}$; $w = 1/\sigma^2(|F_o|)$.

were performed with the use of standard H cells and a platinum-gauze electrode on solutions that were deaerated by purging with dinitrogen gas. Potential control was maintained with a Bioanalytical Systems Inc. SP-2 potentiostat. ^{1}H NMR spectra were recorded on a Varian XL-200 spectrometer. Resonances were referenced internally to the residual protons in the incompletely deuteriated solvent. ^{31}P{^{1}H} NMR spectra were obtained on a Varian XL-200 spectrometer. An internal deuterium lock and an external reference, 85% H$_3$PO$_4$, were used. Conductivity measurements were performed on acetone solutions of the samples at a concentration of ca. 1.0 × 10^{-3} M. Measurements were made on an Industrial Instruments Inc. Model RC-16B2 conductivity bridge. EPR spectra of CH$_2$Cl$_2$ glasses were recorded at ca. −160 °C with a Varian E-109 spectrometer.

Elemental microanalyses were performed by Dr. H. D. Lee of the Purdue University Microanalytical Laboratory.

Synthesis of [Re(acac)$_2$(PPh$_3$)$_2$]PF$_6$ (1). A solution of [ReH(acac)$_2$(PPh$_3$)$_2$]PF$_6$ (0.100 g, 0.095 mmol) and NOPF$_6$ (0.017 g, 0.097 mmol) in 5 mL of acetone was stirred for 10 min. A large excess of diethyl ether (100 mL) was added to the orange solution. The orange precipitate was filtered off, washed with ether, and dried under vacuum; yield 0.063 g (63%). Anal. Calcd for C$_{46}$H$_{44}$F$_6$O$_4$P$_3$Re: C, 52.42; H, 4.22. Found: C, 52.78; H, 4.51.

X-ray Analysis. Orange crystals of [Re(acac)$_2$(PPh$_3$)$_2$]PF$_6$ (**1**) were obtained by recrystallization of the crude product from deoxygenated THF/heptane. The structure of **1** was determined by application of standard procedures. The basic crystallographic parameters for this complex are listed in Table I. The cell constants are based on 25 reflections with $20 < \theta < 22°$. Three standard reflections were measured after every 5000 s of beam exposure during data collection. Calculations were performed on a MicroVAX II computer using the Enraf-Nonius structure determination package. The crystal was found to belong to the monoclinic space group $P2_1/c$ (No. 14). Lorentz and polarization corrections were applied to the data. The structure was solved by the use of the Patterson heavy-atom method, which revealed the position of the Re atom. The remaining non-hydrogen atoms were located in succeeding difference Fourier syntheses. An empirical absorption correction was applied,[2] the linear absorption coefficient being 29.13 cm^{-1}. No corrections for extinction were applied. The structure was refined by the full-matrix least-squares method, where the function minimized was $\sum w(|F_o| - |F_c|)^2$, where w is the weighting factor defined as $w = 1/\sigma^2(F_o)$. Hydrogen atoms were not included. All non-hydrogen atoms were refined anisotropically; corrections for anomalous scattering were applied to these atoms.[3] The largest peak in the final difference Fourier map was 0.55 e/Å^3 and did not appear to be of any chemical significance.

Positional parameters and their errors for the non-phenyl group atoms of the compound are listed in Table II. Important intramolecular bond distances and angles are given in Table III. Tables giving full details of the crystal data and data collection parameters (Table S1), a listing of the positional parameters for the phenyl group carbon atoms (Table S2), the thermal parameters (Table S3), and complete listings of bond distances (Table S4) and bond angles (Table S5) are available as supplementary material.

Table II. Positional Parameters and Equivalent Isotropic Displacement Parameters (Å^2) for Non-Phenyl Group Atoms of **1** and Their Estimated Standard Deviations^a

atom	x	y	z	B, Å^2
Re	0.08802 (2)	0.24058 (1)	0.06338 (1)	2.415 (4)
P(1)	0.0408 (1)	0.19666 (7)	−0.04325 (7)	2.71 (3)
P(2)	−0.0993 (1)	0.30044 (8)	0.09319 (7)	2.95 (3)
O(12)	0.1669 (4)	0.2657 (2)	0.1505 (2)	3.22 (8)
O(14)	0.1490 (4)	0.3294 (2)	0.0311 (2)	3.46 (9)
O(22)	0.0427 (4)	0.1527 (2)	0.1032 (2)	3.00 (8)
O(24)	0.2638 (3)	0.2013 (2)	0.0531 (2)	3.35 (9)
C(11)	0.3191 (8)	0.3059 (5)	0.2256 (4)	6.5 (2)
C(12)	0.2544 (6)	0.3096 (4)	0.1605 (3)	4.3 (2)
C(13)	0.2873 (6)	0.3596 (4)	0.1170 (3)	4.4 (2)
C(14)	0.2306 (6)	0.3693 (3)	0.0582 (3)	3.9 (1)
C(15)	0.2612 (8)	0.4314 (4)	0.0193 (4)	6.0 (2)
C(21)	0.0540 (7)	0.0530 (3)	0.1648 (3)	4.6 (2)
C(22)	0.1197 (6)	0.1088 (3)	0.1297 (3)	3.4 (1)
C(23)	0.2456 (6)	0.1089 (3)	0.1254 (3)	3.9 (1)
C(24)	0.3097 (6)	0.1528 (3)	0.0862 (3)	3.9 (1)
C(25)	0.4481 (7)	0.1420 (5)	0.0801 (4)	7.5 (2)
P(100)	0.4684 (2)	0.4955 (1)	0.7784 (1)	4.91 (4)
F(101)	0.3230 (4)	0.4974 (3)	0.7670 (3)	7.8 (1)
F(102)	0.4629 (5)	0.4177 (2)	0.7890 (3)	9.6 (2)
F(103)	0.4785 (6)	0.4829 (4)	0.7053 (3)	10.2 (2)
F(104)	0.4727 (6)	0.5727 (3)	0.7656 (4)	13.6 (2)
F(105)	0.6134 (5)	0.4918 (3)	0.7873 (3)	10.1 (2)
F(106)	0.4592 (7)	0.5078 (5)	0.8497 (3)	14.4 (3)

[a] Values for anisotropically refined atoms are given in the form of the isotropic equivalent thermal parameter defined as $(4/3)[a^2\beta(1,1) + b^2\beta(2,2) + c^2\beta(3,3) + ab(\cos\gamma)\beta(1,2) + ac(\cos\beta)\beta(1,3) + bc(\cos\alpha)\beta(2,3)]$. Data for the phenyl group atoms are available as supplementary material.

Table III. Important Bond Distances (Å) and Bond Angles (deg) for **1**^{a}

Distances			
Re–P(1)	2.439 (1)	O(24)–C(24)	1.272 (7)
Re–P(2)	2.451 (1)	C(11)–C(12)	1.513 (9)
Re–O(12)	2.048 (4)	C(12)–C(13)	1.404 (9)
Re–O(14)	2.003 (4)	C(13)–C(14)	1.370 (9)
Re–O(22)	1.996 (3)	C(14)–C(15)	1.518 (9)
Re–O(24)	2.073 (4)	C(21)–C(22)	1.520 (8)
O(12)–C(12)	1.292 (7)	C(22)–C(23)	1.368 (8)
O(14)–C(14)	1.295 (7)	C(23)–C(24)	1.402 (9)
O(22)–C(22)	1.310 (7)	C(24)–C(25)	1.523 (9)
Angles			
P(1)–Re–P(2)	105.44 (5)	Re–O(22)–C(22)	126.1 (4)
P(1)–Re–O(12)	166.3 (1)	Re–O(24)–C(24)	124.1 (4)
P(1)–Re–O(14)	93.2 (1)	O(12)–C(12)–C(11)	114.9 (6)
P(1)–Re–O(22)	91.9 (1)	O(12)–C(12)–C(13)	124.7 (6)
P(1)–Re–O(24)	85.7 (1)	C(11)–C(12)–C(13)	120.4 (6)
P(2)–Re–O(12)	88.2 (1)	C(12)–C(13)–C(14)	124.9 (6)
P(2)–Re–O(14)	87.4 (1)	O(14)–C(14)–C(13)	125.5 (6)
P(2)–Re–O(22)	95.1 (1)	O(14)–C(14)–C(15)	114.4 (6)
P(2)–Re–O(24)	168.3 (1)	C(13)–C(14)–C(15)	120.1 (6)
O(12)–Re–O(14)	87.8 (2)	O(22)–C(22)–C(21)	112.6 (5)
O(12)–Re–O(22)	86.2 (1)	O(22)–C(22)–C(23)	125.9 (5)
O(12)–Re–O(24)	80.7 (1)	C(21)–C(22)–C(23)	121.5 (5)
O(14)–Re–O(22)	173.5 (1)	C(22)–C(23)–C(24)	124.1 (6)
O(14)–Re–O(24)	88.5 (1)	O(24)–C(24)–C(23)	126.6 (5)
O(22)–Re–O(24)	87.9 (1)	O(24)–C(24)–C(25)	114.8 (6)
Re–O(12)–C(12)	125.5 (4)	C(23)–C(24)–C(25)	118.6 (6)
Re–O(14)–C(14)	127.6 (4)		

[a] Numbers in parentheses are estimated standard deviations in the least significant digits.

Results

The mononuclear Re(III) complex *cis*-[Re(acac)$_2$(PPh$_3$)$_2$]PF$_6$ (**1**) is formed as a major product upon treating the 17-electron monohydride complex [ReH(acac)$_2$(PPh$_3$)$_2$]PF$_6$ with NOPF$_6$ in acetone (or dichloromethane). It is also generated quantitatively by the electrochemical oxidation of [ReH(acac)$_2$(PPh$_3$)$_2$]PF$_6$ in TBAH/CH$_2$Cl$_2$ at a potential of ca. +0.9 V vs. Ag/AgCl. The structural identity of this complex has been established by a single-crystal X-ray structure analysis. Important details of the crystallographic and structural parameters are presented in Tables I–III, while an ORTEP representation of the structure of the cation is given in Figure 1.

Crystals of **1** are stable in air, and the orange-colored solutions of this complex in acetone or dichloromethane also appear to be

---

(2) Walker, N.; Stuart, D. *Acta Crystallogr., Sect. A: Found Crystallogr.* **1983**, *A39*, 158.

(3) (a) Cromer, D. T. *International Tables for X-ray Crystallography*; Kynoch: Birmingham, England, 1974, Vol. IV, Table 2.3.1. (b) For the scattering factors used in the structure solution, see: Cromer, D. T.; Waber, J. T. *Ibid.*; Table 2.2B.

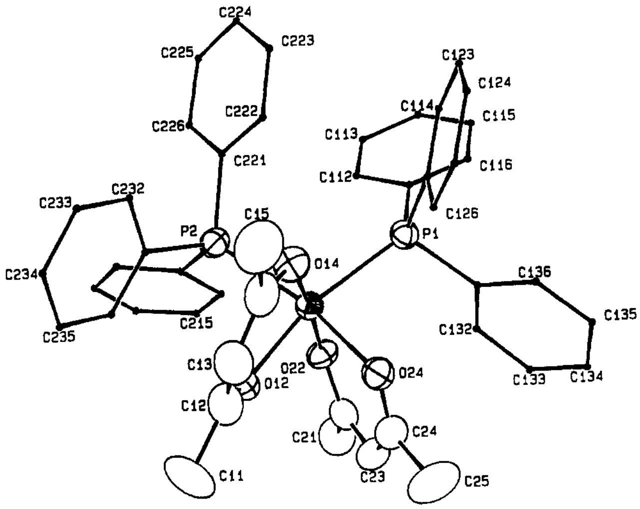

Figure 1. ORTEP representation of the structure of the *cis*-[Re(acac)$_2$(PPh$_3$)$_2$]$^+$ cation of **1** showing the atomic numbering scheme. The thermal ellipsoids are drawn at the 50% probability level except for the carbon atoms of the phenyl rings which are circles of arbitrary radius.

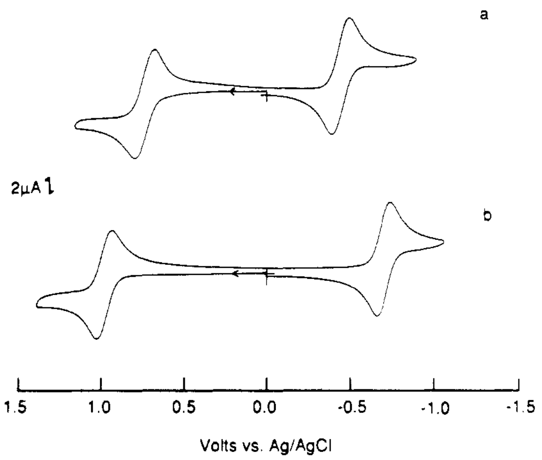

Figure 2. (a) Single-sweep cyclic voltammogram of a solution of [ReH(acac)$_2$(PPh$_3$)$_2$]PF$_6$ in 0.1 M TBAH/CH$_2$Cl$_2$ (a) recorded at 200 mV s^{-1} with a Pt-bead electrode. (b) CV of the solution used in part a following its complete electrolysis at a potential of ca. +0.9 V vs Ag/AgCl.

stable for several days upon exposure to the atmosphere. Conductivity measurements on acetone solutions of **1** ($c_m = 1 \times 10^{-3}$ M) confirm it to be a 1:1 electrolyte ($\Lambda_m = 114\ \Omega^{-1}\ \mathrm{cm}^2\ \mathrm{mol}^{-1}$). Its Nujol mull IR spectrum shows characteristic ν(C$\overset{\cdots}{-}$O) and ν(C$\overset{\cdots}{-}$C) bands of chelating acetylacetonate ligands at 1556 (s) and 1508 (s) cm^{-1}, as well as an intense band at 842 cm^{-1} due to ν(P—F) of [PF$_6$]$^-$. The electronic absorption spectrum of a solution of **1** in CH$_2$Cl$_2$ shows an absorption at $\lambda_{max} = 348$ (ϵ = 760) with an accompanying shoulder at 430 (ϵ = 220).

Compound **1** is paramagnetic (μ_{eff} = 2.4 (±0.1) μ_B) as determined by the Evans method[4] on a dichloromethane solution. Furthermore, the X-band ESR spectrum (−160 °C) of the same solution shows a broad (1.5–4.5 kG), complex signal centered at g = ca. 2.2. The ^{31}P{^{1}H} NMR spectrum (recorded in CD$_2$Cl$_2$) shows only a resonance due to the diamagnetic [PF$_6$]$^-$ anion (δ −144.0, septet), while the ^{1}H NMR spectrum consists of sharp Knight-shifted resonances typical of a paramagnetic octahedral d^4 Re(III) species.[5-8] The phenyl protons of the two PPh$_3$ ligands appear as a doublet and two triplets (δ +9.2 (d), +8.6 (t), and +8.2 (t); $J_{H-H} \simeq 7.5$ Hz) in an intensity ratio of 2:2:1. There are two singlets at δ +8.5 and −10.2 of equal intensity; these are assigned to the protons of the inequivalent methyl groups on the acac ligands (see Figure 1). A singlet at δ +16.8 corresponds to the methyne protons of the acac ligands. All integrations are in accord with the stoichiometry [Re(acac)$_2$(PPh$_3$)$_2$]PF$_6$.

The cyclic voltammogram (CV) of **1** in 0.1 M TBAH/CH$_2$Cl$_2$ shows two reversible processes at $E_{1/2}$ = +0.97 V and $E_{1/2}$ = −0.72 V vs Ag/AgCl, which correspond to a one-electron oxidation and one-electron reduction of the complex, respectively. Upon the electrochemical reduction of **1** at −0.90 V, a yellow species is generated that displays similar electrochemical properties to those of **1**, except that the process at $E_{1/2}$ = −0.72 V is now an oxidation. Attempts to isolate this product (it is, presumably, *cis*-Re(acac)$_2$(PPh$_3$)$_2$) by workup of the solution or by the alternative means of reacting *cis*-[Re(acac)$_2$(PPh$_3$)$_2$]PF$_6$ with the one-electron reductant (η^5-C$_5$H$_5$)$_2$Co were not successful. Also, attempts to obtain it by deprotonation of [ReH(acac)$_2$(PPh$_3$)$_2$]PF$_6$ with the base DBU were likewise unsuccessful.

Discussion

The preparation of the complex ReH(acac)$_2$(PPh$_3$)$_2$ and its oxidation to [ReH(acac)$_2$(PPh$_3$)$_2$]PF$_6$ has been described in a previous report.[1] The cyclic voltammogram of a solution of [ReH(acac)$_2$(PPh$_3$)$_2$]PF$_6$ in 0.1 M TBAH/CH$_2$Cl$_2$ shows a reversible process at $E_{1/2}$ = +0.85 V (an oxidation) and one at $E_{1/2}$ = −0.44 V (a reduction) vs Ag/AgCl (Figure 2). Oxidation of this complex at a potential of ca. +0.9 V does not give the rhenium(V) hydrido complex [ReH(acac)$_2$(PPh$_3$)$_2$]$^{2+}$ but instead affords the Re(III) complex *cis*-[Re(acac)$_2$(PPh$_3$)$_2$]PF$_6$. The CV of the solution that results is shown in Figure 2. This conversion proceeds essentially quantitatively, based upon peak current measurements. The same reaction occurs when NOPF$_6$ is used as the chemical oxidant. The deprotonation of [ReH(acac)$_2$(PPh$_3$)$_2$]$^{2+}$ cannot be reversed by the treatment of *cis*-[Re(acac)$_2$(PPh$_3$)$_2$]PF$_6$ with HPF$_6$, and it seems reasonable to conclude that the formation of *cis*-[Re(acac)$_2$(PPh$_3$)$_2$]PF$_6$ does indeed proceed through a coupled electrochemical oxidation/chemical deprotonation involving the putative species [ReH(acac)$_2$(PPh$_3$)$_2$]$^{2+}$.

The ORTEP representation of the structure of the *cis*-[Re(acac)$_2$(PPh$_3$)$_2$]$^+$ cation of **1** is shown in Figure 1 while bond distance and bond angle data are given in Table III. There is a striking similarity between the ReO$_4$P$_2$ coordination sphere of this complex and those of the hydride precursors ReH(acac)$_2$(PPh$_3$)$_2$ and [ReH(acac)$_2$(PPh$_3$)$_2$]PF$_6$.[1] Clearly, the conversion of [ReH(acac)$_2$(PPh$_3$)$_2$]$^{2+}$ to *cis*-[Re(acac)$_2$(PPh$_3$)$_2$]$^+$ occurs with a minimum of structural reorganization. Most significant is the striking similarity between the crystallographic parameters of **1** (Table I) and those of [ReH(acac)$_2$(PPh$_3$)$_2$]PF$_6$ (see Table I of ref 1).[9] While the Re-P distances of **1** (2.439 (1) and 2.451 (1) Å) are on average longer than those of [ReH(acac)$_2$(PPh$_3$)$_2$]PF$_6$ (2.396 (3) and 2.439 (3) Å), the Re–O distances are very similar, being in the range 1.996 (3)–2.073 (4) Å for **1** versus 2.013 (6)–2.092 (7) Å for [ReH(acac)$_2$(PPh$_3$)$_2$]PF$_6$. The trans O–Re–O angles are also similar (O(14)–Re–O(22) = 173.5 (1)° for **1** versus the corresponding angle of 169.3 (3)° for [ReH(acac)$_2$(PPh$_3$)$_2$]PF$_6$), as are the corresponding pair of cis angles (i.e. O(12)–Re–O(24) for **1**), which are 80.7 (1) and 80.9 (3)°, respectively. The decrease in the P–Re–P angle from 110.35 (4)° in [ReH(acac)$_2$(PPh$_3$)$_2$]PF$_6$ to 105.44 (5)° in **1** reflects the absence of a hydride ligand in **1** since in [ReH(acac)$_2$(PPh$_3$)$_2$]PF$_6$ this ligand is located in the coordination sphere between the phosphine ligands and is responsible, in part, for the opening up of this angle.

Several other six-coordinate mononuclear acetylacetonate complexes of rhenium(III) have been structurally character-

---

(4) Evans, D. F. *J. Chem. Soc.* **1959**, 2003.

(5) Cameron, C. J.; Tetrick, S. M.; Walton, R. A. *Organometallics* **1984**, *3*, 240.

(6) Rossi, R.; Duatti, A.; Magon, L.; Casellato, U.; Graziani, R.; Toniolo, L. *J. Chem. Soc., Dalton Trans.* **1982**, 1949.

(7) Gunz, H. P.; Leigh, G. J. *J. Chem. Soc. A* **1971**, 2229.

(8) Randall, E. W.; Shaw, D. *J. Chem. Soc. A* **1969**, 2867.

(9) These parameters are so similar that during the early stages of the structure solution of *cis*-[Re(acac)$_2$(PPh$_3$)$_2$]PF$_6$ we thought we might have inadvertently used a crystal of [ReH(acac)$_2$(PPh$_3$)$_2$]PF$_6$. However, we confirmed that this was not the case by characterizing this particular crystal by the use of cyclic voltammetry. It was unambiguously proven to be *cis*-[Re(acac)$_2$(PPh$_3$)$_2$]PF$_6$.

ized.[10-12] For the complexes $Re(acac)_2Cl_2$,[10] $ReCl_2(acac)(PPh_3)_2$,[11] and $[Ph_4As][Re(acac)_2Cl_2]$,[12] the X-ray structural analyses were carried out on the trans isomers (trans phosphines in the case of $ReCl_2(acac)(PPh_3)_2$). Therefore, the geometry of these complexes more closely approaches that of regular octahedral species, than does that of **1**. The bond angles and bond lengths of the acac ligands in these reported structures are very similar to those of **1**. The Re–P bond lengths in *trans*-$ReCl_2(acac)(PPh_3)_2$ (2.485 (4) and 2.469 (4) Å)[11] are also similar to those of **1**.

Acknowledgment. Support from the National Science Foundation, through Grant No. CHE88-07444 to R.A.W. and Grant No. CHE86-15556 for the purchase of the MicroVAX II computer and diffractometer, is gratefully acknowledged. We also acknowledge the National Institutes of Health (Grant No. RR-01077) and the National Science Foundation (Grant No. 87-14258) for funds for the purchase of the NMR spectrometers.

Supplementary Material Available: Tables giving full details of the crystal data and data collection parameters (Table S1), positional parameters for the phenyl group carbon atoms (Table S2), and the thermal parameters (Table S3) and complete listings of bond distances (Table S4) and bond angles (Table S5) (12 pages); tables of observed and calculated structure factors (34 pages). Ordering information is given on any current masthead page.

(10) Brown, I. D.; Lock, C. J. L.; Wan, C. *Can. J. Chem.* **1973**, *51*, 2073.
(11) Brown, I. D.; Lock, C. J. L.; Wan, C. *Can. J. Chem.* **1974**, *52*, 1704.
(12) Lock, C. J. L.; Murphy, C. N. *Acta Crystallogr., Sect. B: Struct. Crystallogr. Cryst. Chem.* **1979**, *B35*, 951.

Contribution from the Institute of Agricultural Chemistry,
University of Bologna, Viale Berti Pichat 10,
40127 Bologna, Italy, Bruker GmbH, Silberstreifen,
D-7512 Rheinstetten 4, Federal Republic of Germany,
and Department of Chemistry, University of Florence,
Via Gino Capponi 7, 50121 Florence, Italy

Application of 2D NMR Techniques to Paramagnetic Systems

Claudio Luchinat,*[†] Stefan Steuernagel,[‡] and Paola Turano[§]

Received November 21, 1989

Two-dimensional NMR experiments on paramagnetic systems have been seldomly attempted due to their intrinsic difficulties. Paramagnetic systems are characterized by short nuclear relaxation times due to magnetic coupling of nuclear spins with unpaired electrons. 2D spectroscopy in general requires the application of two or more pulses interleaved by variable and fixed delays to allow the development of the coherences required by each particular experiment. During these times before the acquisition, nuclear relaxation processes cause the overall magnetization to relax back to its equilibrium value. As a consequence, the intensities of the cross peaks are predicted to be much smaller than in slow-relaxing systems.

The most common 2D experiments, COSY and NOESY, suffer from additional drawbacks: the fractional intensities of NOESY cross peaks, even under ideal conditions, are of the order of the steady-state NOE effect, $\eta = \sigma/\rho$, which, especially in small paramagnetic molecules, is always much smaller than unity due to the small σ and large ρ values. COSY cross peaks always show antiphase structure within the multiplet, therefore leading to dramatic cancellation of intensities everytime the J splitting is not resolved; in paramagnetic systems this almost always happens. Despite these difficulties a few COSY and NOESY experiments on paramagnetic molecules with relatively long nuclear T_1 values have been reported.[1-5]

These disadvantages of COSY and NOESY experiments, however, are less severe in other 2D spectroscopies. For instance, chemical exchange effects detected through NOESY type experiments (EXSY) do not have the intrinsic reduced sensitivity of NOE effects. EXSY experiments have been already successfully performed on paramagnetic substances.[3,4,6] Scalar J couplings detected through TOCSY type experiments[7] create cross peaks with in-phase structure of multiplets. This kind of experiment increases the sensitivity for small J values[8,9] and should therefore be more appropriate than COSY experiments in paramagnetic systems.

Experimental Section

The complex [*N*,*N*'-(4-methyl-4-azaheptane-1,7-diyl)bis(5-chlorosalicylideneaminato)]nickel(II) (5-Cl-NiSAL-MeDPT) was prepared as previously reported.[10] The ^1H NMR spectra in $CDCl_3$ were recorded at room temperature on a Bruker MSL300 instrument with a fast low-dynamic range digitizer to cover the entire spectral region. T_1 measurements, in order to minimize the deviation of the pulses from the ideal behavior,[11] were performed with a standard inversion recovery sequence with a composite 180° pulse[12] on four different regions of the spectrum. For HOHAHA experiments the MLEV17 mixing sequence[9] was employed in order to efficiently spin-lock transverse magnetization. EXSY experiments were performed by using the standard phase-sensitive NOESY pulse sequence.

Results and Discussion

We have decided to test the feasibility of HOHAHA and EXSY experiments on the paramagnetic complex 5-Cl-NiSAL-MeDPT. This complex is a member of a family of complexes with general formula reported as follows:

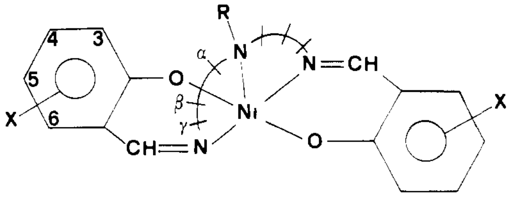

R = CH_3,H

It is known to give rise to well-resolved NMR spectra spread over a very large chemical shift range and to show separate signals for each of the 23 protons except the methyl group. This is due to the fact that the molecule is chiral and lacks a C_2 axis because of the substituent on the apical nitrogen. This also makes the methylene protons of the propylene chains diastereotopic and therefore not equivalent. The assignment of the signals to the various types of protons has been already performed.[13] It was also proposed, but never demonstrated, that interconversion of one enantiomer into the other was possible, although slow on the NMR time scale because it requires breaking of coordination bonds.[14] The choice of the 5-Cl derivative allows us to eliminate the overlap between the H5 proton signals of the ring and the β-CH_2 proton signals of the propylene chains. The spectrum of 5-Cl-NiSAL-MeDPT is shown in Figure 1, together with the assignment. It should be stressed that, due to the large line widths, no J splitting is resolved for any of the ^1H signals.

---

[*] To whom correspondence should be addressed.
[†] University of Bologna.
[‡] Bruker GmbH.
[§] University of Florence.

(1) Peters, W.; Fuchs, M.; Sicius, H.; Kuchen, W. *Angew. Chem.* **1985**, *24*, 231.
(2) Yu, C.; Unger, S. W.; La Mar, G. N. *J. Magn. Reson.* **1986**, *67*, 346.
(3) Jenkis, B. G.; Lauffer, R. B. *J. Magn. Reson.* **1988**, *80*, 328.
(4) Jenkins, B. G.; Lauffer, R. B. *Inorg. Chem.* **1988**, *27*, 4730.
(5) Emerson, S. D.; La Mar, G. N. *Biochemistry* **1990**, *29*, 1545.
(6) Santos, H.; Turner, D. L.; Xavier, A. V. *J. Magn. Reson.* **1984**, *59*, 177.
(7) Braunschweiler, L.; Ernst, R. R. *J. Magn. Reson.* **1983**, *53*, 521.
(8) Davis, D. G.; Bax, A. *J. Am. Chem. Soc.* **1985**, *107*, 2820.
(9) Bax, A.; Davis, D. G. *J. Magn. Reson.* **1985**, *65*, 355.
(10) Sacconi, L.; Bertini, I. *J. Am. Chem. Soc.* **1966**, *88*, 5180.
(11) Bertini, I.; Luchinat, C. *NMR of Paramagnetic Molecules in Biological Systems*; Benjamin Cummings: Boston, MA, 1986.
(12) Levitt, M. H.; Freeman, R. *J. Magn. Reson.* **1979**, *33*, 473.
(13) La Mar, G. N.; Sacconi, L. *J. Am. Chem. Soc.* **1967**, *89*, 2282.
(14) Bertini, I.; Sacconi, L.; Speroni, P. *Inorg. Chem.* **1972**, *11*, 1323.

0020-1669/90/1329-4351$02.50/0